TECTONO-MAGMATIC SIGNIFICANCE OF THE PILLOW BASALTS FROM THE OPHIOLITIC MÉLANGE OF THE DINARIDES

Sanja Šuica[*,✉], **Boško Lugović**[**†] and **Duje Kukoč**[***,°]

* *Rock and Fluid Research Department, INA-Industrija nafte, Zagreb, Croatia.*
** *Faculty of Mining, Geology and Petroleum Engineering, University of Zagreb, Croatia.*
*** *Institut des Sciences de la Terre, Université de Lausanne, Géopolis, Switzerland.*
° *Department of Geology, Croatian Geological Survey, Zagreb, Croatia.*
✉ *Corresponding author, e-mail: sanja.suica@ina.hr*

Keywords: *Basalts; radiolarians; ophiolitic mélange; Triassic; Jurassic; Dinarides.*

ABSTRACT

The remnants of the Neotethyis in the area of the Dinarides are represented by numerous ophiolitic complexes and associated mélanges. This paper presents the results of a regional study of pillow basalts and related pelagic sediments. The study area stretches from the northwestern Croatia across the Bosnia and Herzegovina to the southern Serbia. Basaltic rocks are divided into four groups: within-plate alkaline basalts, CAB, E-MORB, IAT and BABB basalts. Pelagic sediments related to basalts with BABB geochemical characteristics yielded Middle Jurassic age. Data presented in this paper as well as previously published data, allowed recognition of two phases of ocean development: (1) the Middle Triassic terminal phase of intracontinental rifting with alkaline basalt, CAB and E-MORB magmatism, (2) compressional phase resulting in IAT and BABB magmatism during Middle and Late Jurassic. These groups are compared to similar rocks in Hellenides. The paper presents the insight into the oceanic evolution of the Neotethys in the Dinaride area - from continental break-up and initiation of sea-floor spreading to compressional stage.

INTRODUCTION

Ophiolitic mélanges are common in orogenic belts created by accretionary and collisional processes. These chaotic tectono-sedimentary units are made up of blocks of various lithologies embedded most commonly in shaley or sandy matrix. Among the blocks of different ages and origins, the pillow basalts represent important lithologies that represent remnants of crustal sequences originated in a variety of oceanic geotectonic settings. Because most of the oceanic crust is consumed during subduction, these ophiolitic fragments offer valuable information about different stages of oceanic evolution (e.g. Pearce, 2008; Dilek and Furnes, 2011; Saccani et al., 2011). Basaltic blocks are often associated with pelagic sediments deposited on the newly formed crust shortly after its formation. These sediments make a potential source for biostratigraphic dating based on their planktonic fossils, most commonly radiolarians, thus providing a crucial age determination of ocean-floor basalts (e.g. Gawlick et al., 2016).

The outcrops of the ophiolitic mélange in the Dinarides are part of the larger chain of ophiolite occurrences stretching from northwestern Croatia to the southern Greece (e.g. Schmid et al., 2008, Fig. 1). The origin of these ophiolites is a subject of a long lasting debate. Open questions include number and location of ocean basins, timing of their closure and direction of emplacement of the ophiolites (e.g. Saccani et al., 2011; Ferrière et al., 2012; 2016; Robertson, 2012; Bortolotti et al., 2013; Gawlick et al., 2016). Extensive petrological, geochemical and biostratigraphic studies have been done on ophiolitic mélanges in Albania and Greece (e.g. Jones and Robertson, 1991; Saccani et al., 2003; 2011; Bortolotti et al., 2004; 2009; 2013; Saccani and Photiades, 2005; Chiari et al., 2012), however data from the Dinarides are still relatively sparse. So far, data exist from the ophiolitic mélange in Croatia (Slovenec and Lugović, 2009; 2012; Slovenec et al., 2010; 2011; Lugović et al., 2015; Šegvić et al., 2016), Bosnia and Herzegovina (Šegvić, 2010; Trubelja et al., 1995) and Serbia (Chiari et al., 2011; Gawlick et al., 2016). In addition, several biostratigraphic radiolarian data have been published from the ophiolite mélange of the Dinarides (Obradović and Goričan, 1988; Halamić and Goričan, 1995; Halamić et al., 1999; Goričan et al., 2005; Djerić and Gerzina, 2008; Gawlick et al., 2009; 2016; Vishnevskaya et al., 2009; Djerić et al., 2010; Chiari et al., 2011; Šegvić et al., 2014; Gawlick et al., 2016).

The aim of this paper is to present new geochemical petrological and biostratigraphic data on basalts and radiolarites from ophiolitic mélanges of the Dinarides, sampled from northwestern Croatia, across Bosnia and Herzegovina to southern Serbia. The sampled basalts are divided into four groups based on geochemical characteristics, representing different stages of the oceanic evolution. These data provide new insights into the tectono-magmatic evolution of the basalts from the Dinaric part of Neotethys.

REGIONAL GEOLOGICAL SETTING

Ophiolites and associated ophiolitic mélanges occur in two distinct belts in the Dinarides: the more external Dinaridic Ophiolite Belt (Pamić et al., 2002; Karamata, 2006) or Central Dinaridic ophiolite belt (Lugović et al., 1991) and more internal Western Vardar ophiolites (Karamata, 2006), or Inner Dinaridic ophiolite belt (Lugović et al. 1991), External Vardar Subzone (Dimitrijević, 1997), Vardar Zone (Pamić et al., 2002). The external belt is characterized by lherzolites and rare occurrence of harzburgites and extrusive rocks (Lugović et al., 1991; Robertson et al., 2009). Harzburgites predominate in the internal belt with abundant occurrences of extrusive rocks with suprasubduction geochemical signatures (Spray et al., 1984; Lugović et al., 1991; Robertson et al., 2009). Some authors (e.g. Spray et al., 1984; Lugović et al., 1991; Karamata, 2006; Robertson et al., 2009; 2013) tried to explain the differences of the

belts by interpreting them as being derived from two distinctive oceanic domains. However, most of the authors (e.g. Bernoulli and Laubscher, 1972; Baumgartner et al., 1995; Pamić et al., 2002; Bortolotti et al., 2004; 2013; Bortolotti and Principi, 2005; Schmid et al., 2008; Chiari et al., 2011; Ferrière et al., 2012; 2016) agree that these belts represent a single ophiolitic thrust sheet derived from a single oceanic basin, i.e. Maliac-Meliata-Vardar. According to the terminology proposed by Schmid et al. (2008) both belts are referred to as the Western Vardar Ophiolitic Unit. To the south this unit includes the Mirdita ophiolites in Albania (e.g. Bortolotti et al., 1996; Gawlick et al., 2008) and several ophiolite complexes further south in Greece (e.g. Schmid et al., 2008; Ferrière et al., 2016).

Geodynamic evolution based on one ocean model is reconstructed mostly on the basis of data from the Albanides and Hellenides (summarized in Schmid et al., 2008; Chiari et al., 2011; Bortolotti et al., 2013; Ferrière et al., 2016) and includes rifting in the Middle Triassic and opening phase during Late Triassic and Early Jurassic. Change to convergent regime occurred in the Early to early Middle Jurassic (Bortolotti et al., 2013). Convergence resulted in a destruction of the subducting plate and formation of supra-subduction zone type (SSZ) crust (e.g. Ferrière et al., 2016). Shortly after their formation, in Middle to Late Jurassic, supra-subduction ophiolites were emplaced on the adjacent passive continental margin of Adria. The obduction was associated with development of metamorphic sole and mélange at the base of the ophiolite nappe. Some authors (e.g. Bortolotti et al., 2013) claim that latermost Jurassic is the time all oceanic areas were closed, so the continental collision started between latemost Late Jurassic and the earliest Cretaceous. However, the existence of the Cretaceous oceanic lithosphere in northern Bosnia and Herzegovina (e.g. Ustaszewski et al., 2009) and NW Croatia (Šegvić et al., 2016), as well as various subduction related magmatic, metamorphic and sedimentary units of Cretaceous and Paleogene age in Bosnia and Herzegovina and Serbia (summarized in Ustaszewski et al., 2010) implies that continental collision was not synchronous in all oceanic domains.

Ophiolitic mélange in the Dinarides

Ophiolitic mélange (Diabase - Radiolarite Formation of Ćirić and Karamata, 1960 or olistostrome mélange of Dimitrijević and Dimitrijević, 1973) is widespread in the Dinarides. Structurally, it is positioned bellow the metamorphic sole at the base of the ophiolitic nappe (Saccani and Photiades, 2005; Schmid et al., 2008). The sub-ophiolitic mélange contains a mixture of lithologies that were mechanically scraped off the lower plate during convergence as well as gravitationally emplaced slide-blocks derived from the upper plate (Bortolotti et al., 1996; Schmid et al., 2008; Chiari et al., 2011). Blocks up to a km size were emplaced in sedimentary matrix composed of shales, coarse-grained arenites, pebbly mudstones and pebbly sandstones (Babić et al., 2002; Chiari et al., 2011). Blocks of Triassic platform and pelagic deposits from the Adria continental margin predominate in the mélange (Goričan et al., 1999; 2005; Dimitrijević et al., 2003; Chiari et al., 2011; Gawlick et al., 2016). The oceanic lihologies include amphibolites, serpentinized peridotites, gabbros, basalts and cherts (Chiari et al., 2011). Geochemical characteristics of basaltic blocks indicate a presence of basalts formed at the mid-ocean ridge and in supra-subduction setting (Chiari et al., 2011; Slovenec et al., 2011), as well as those formed in intracontinental rift setting (Slovenec et al., 2011). Middle to Late Triassic radiolarites associated with pillow basalts within ophiolitic mélange have been found in several places (Obradović and Goričan, 1988; Goričan et al., 1999; Vishnewskaya et al., 2009; Gawlick et al., 2009; 2016). Middle Jurassic radiolarites have been found in ophiolitic mélanges as slide blocks (Obradović and Goričan, 1988; Gawlick et al., 2009; Vishnevskaya et al., 2009; Djerić et al., 2010; Chiari et al., 2011; Šegvić et al., 2014).

SAMPLING LOCATIONS

Six areas were sampled during this research. In total, 25 samples were taken for geochemical and micropaleontological analysis (Table 1). Study area includes different sectors of Western Vardar Ophiolitic Unit (Schmid et al., 2008), stretching from northwestern Croatia (Kalnik, Medvednica and Banija ophiolitic mélange) through Bosnia and Herzegovina (Krivaja-Konjuh and Zvornik ophiolitic mélange) to southern Serbia (Zlatibor, Maljen and Kopaonik ophiolitic mélange). Samples include 17 pillow basalts from ophiolitic mélange, sampled along with interpillow sediments (eight samples), where it was possible, two samples of radiolarite blocks found in the vicinity of sampled basalts, two samples of pillow basalts from the ophiolitic complex, along with one sample of radiolarite in stratigraphic succession with basalt. The sampling positions are shown in Fig. 1.

Table 1 - Sampling locations.

Locality	Sample	Lithology
Kalnik ophiolitic mélange	zmdt-01a-c	basalt
	zmdt-01	limestone (interpillow matrix)
	zmdt-02	basalt
Medvednica ophiolitic mélange	zmdt-03	basalt
	zmdt-04	basalt
Banija ophiolite mélange	doz-13	basalt
Krivaja-Konjuh ophiolitic mélange	doz-06a	chert (interpillow matrix)
	doz-06b-d	basalt
	doz-08	chert (block)
	doz-09	chert (interpillow matrix)
	doz-09a-b	basalt
	doz-10	chert (block)
Krivaja-Konjuh ophiolitic complex	dub-02	basalt
	doz-11a	chert (stratigraphic succession)
	doz-11b	basalt
Zvornik ophiolitic mélange	doz-04a	basalt
	doz-04b	chert (interpillow matrix)
Zlatibor ophiolitic mélange	doz-03a	basalt
	doz-03b	chert (interpillow matrix)
Kopaonik ophiolitic mélange	wvz-02a	basalt
	wvz-02b	chert (interpillow matrix)
Maljen ophiolitic mélange	wvz-03a	basalt
	wvz-03b	chert (interpillow matrix)
	wvz-04a	basalt
	wvz-04b	chert (interpillow matrix)

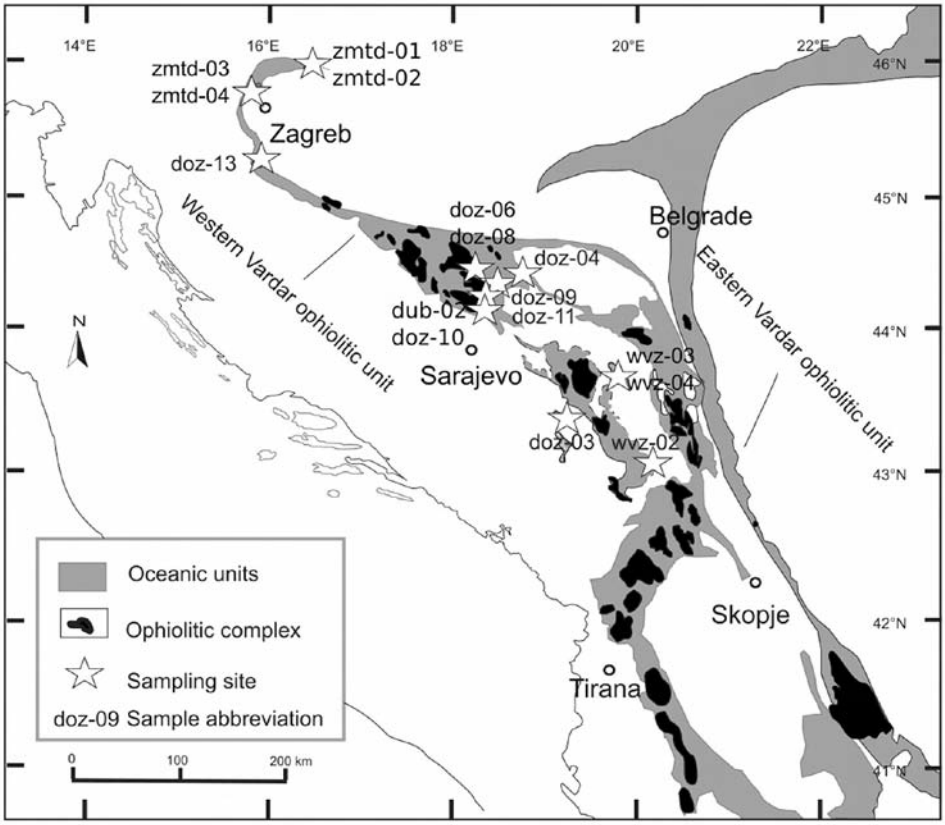

Fig. 1 - Oceanic units in the area of the Dinarides modified after Schmid et al. (2008), with position of ophiolitic complexes after Lugović et al. (1991). The sampling sites are marked with star.

METHODS

Mineral chemistry for 19 samples was obtained with CAMECA SX51 electron microprobe equipped with five wavelength-dispersive spectrometers, at the Institut für Geowissenschaften, Universität Heidelberg. Measurements were performed under conditions of 15 kV of accelerating voltage, 20 nA beam current, ~ 1 μm (10 μm for plagioclase) beam diameter. Standards were natural minerals - oxides (corundum, hematite, spinel, rutile) and silicates (albite, orthoclase, anorthite and wollastonite). Raw data were corrected for matrix effects with the PAP algorithm implemented by CAMECA. Mineral formulas were calculated by using a software package designed by Hans-Peter Meyer (Institut für Geowissenschaften, Universität Heidelberg).

Whole rock chemical analysis was performed on 19 samples at the ACME Analytical Laboratories Ltd., Vancouver, Canada. The samples were analysed by ICP-ES for major and some trace elements (Ba, Sr, Zr, Y, Nb, Sc, Ni), while REE, Cs, Th, U, Ta, Nb, Hf, V, Zr, Y, Rb, Ba, Sr were analysed by ICP-MS. The rocks were analysed after 4-acid digestion (HNO_3-$HClO_4$-HF and HCl) of 0.25 g sample, while the REE were analysed after $LiBO_2/Li_2B_4O_7$ fusion and nitric acid digestion of a 0.1 g sample. International mafic rocks were used as reference materials. Accuracy for ICP-ES analyses is better than 3% for major elements and 5% for trace elements, respectively. Detection limits for trace elements are: Ni, Co, 20 ppm; Ba, Nb, Zn, Zr = 5 ppm; Sc = 1 ppm. Accuracy for ICP-MS analyses ranges from 2 to 8%. Detection limits for trace elements are: V = 8 ppm; Ba, Sn, Zn = 1 ppm; Th, Nb, Ta, Hf, Y, U, Zr, Pb, Rb, Cs; = 0.1 ppm; for REE: Nd = 0.3 ppm; La, Ce = 0.1 ppm; for the rest of the REE is better than 0.05 ppm.

PETROGRAPHY AND MINERAL CHEMISTRY

The extrusive rocks analyzed in this paper are divided in five groups, based on geochemical characteristics. They are affected by polyphase hydrothermal alteration, but igneous textures are well preserved in all samples (Figs. 2 and 3). The primary mineral assemblage is composed of plagioclase, clinopyroxene, Fe-Ti oxide, ± spinel, ± volcanic glass. The most important secondary minerals are albite and chlorite, accompanied by actinolite, pumpellyite, prehnite, analcime, epidote and titanite. Analyzed rocks are exclusively pillow basalts, so the texture of the selected specimen depends on its position within the pillow. Aphyric varieties often contain skeletal clinopyroxene phenocrysts, dendritic and variolitic clinopyroxene as well as variolitic aggregates of plagioclase in the groundmass, indicating an extremely high cooling rate.

Group 1: Clinopyroxene-phyric to aphyric, sporadically hypohialine basalts contain calcite and subordinate chlorite amygdules (Fig. 2a). The groundmass is composed of acicular microliths of plagioclase and clinopyroxene with devitrified glass infillings (Fig. 3a). Plagioclase is altered to albite, rarely accompanied by sericite. Clinopyroxene is slightly or completely replaced by chlorite or actinolite. Fe-Ti oxide is altered to titanite, while volcanic glass is altered to epidote and chlorite.

Group 2: Aphyric, amygduloidal basalts are characterized by high content (up to 30%) of calcite and chlorite amygdules (Fig 2 b). The groundmass is composed of devitrified glass, plagioclase microliths and dendritic clinopyroxene. Plagioclase is altered to albite and sericite, clinopyroxene to chlorite and Fe-Ti oxide to titanite.

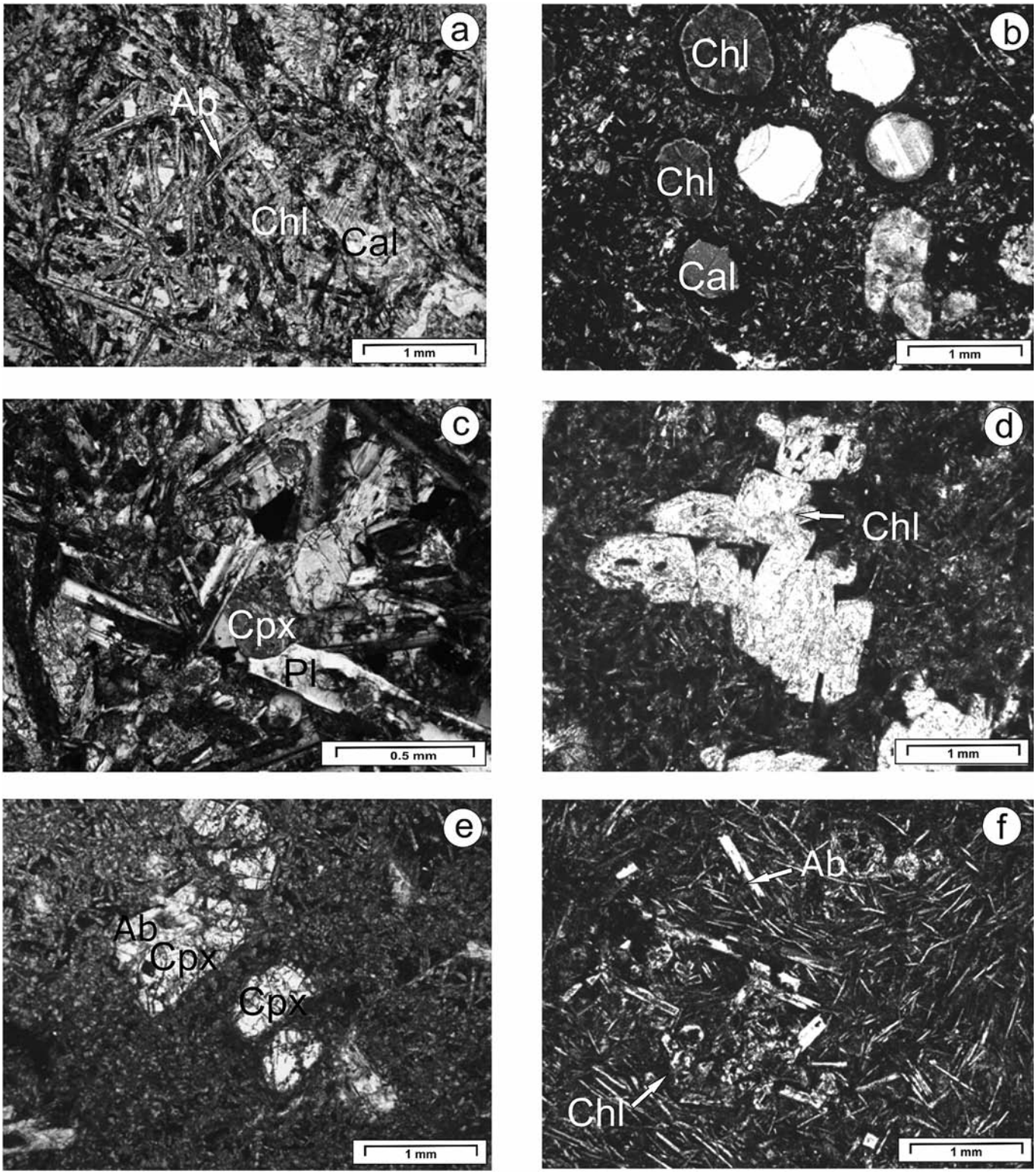

Fig. 2 - Microphotographs of pillow basalts from the Dinaridic ophiolitic mélange. For details see text. Cpx- clinopyroxene, Ab- albite; Pl- plagioclase; Chl- chlorite; Act- actinolite; Cal- calcite.

Group 3: Oligophyric to ophitic basalts show a large variety of microstructures (Figs. 2c; 3b, c). Primary mineral assemblage includes the bright pink clinopyroxene grains, elongated to acicular plagioclase, Ti-magnetite ± volcanic glass. Plagioclase occurs as the compositionally homogenous labradorite (An_{58}) or normally zoned labradorite (An_{53}) to andesine (An_{47}). It is partially replaced by albite and sporadically by analcime. Clinopyroxene is occasionally altered to chlorite, epidote and analcime, while Ti-magnetite (2.95-18.53 wt.% TiO_2) is partially replaced by titanite.

Group 4: Porphyric (Figs. 2d, e and 3d, e) and aphyric basalts. Primary assemblage includes clinopyroxene, plagioclase and Ti-magnetite (16.99 wt.% TiO_2) ± volcanic glass.

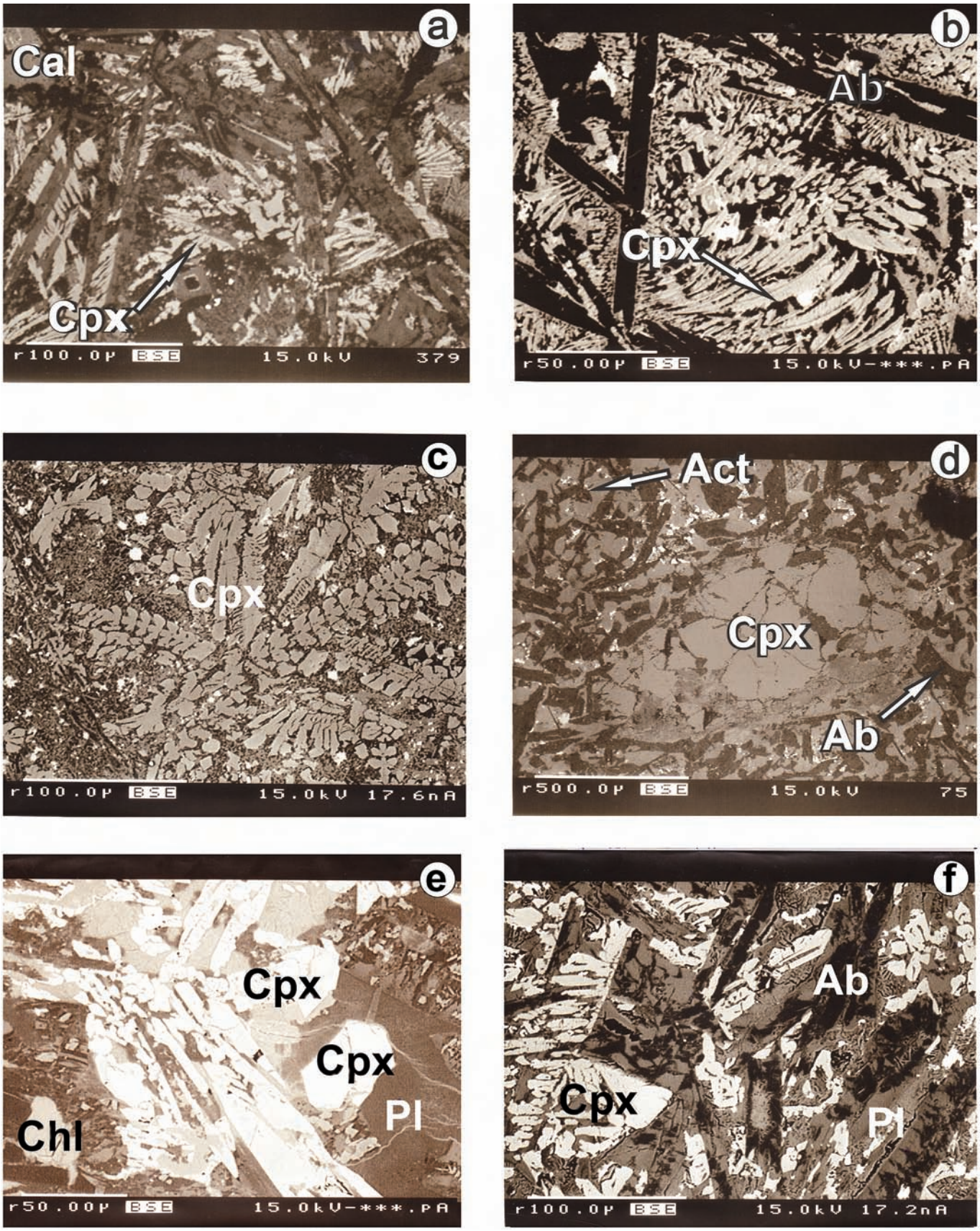

Fig. 3 - EMPA-BSE (electron microprobe analyser-back scattered electron) microphotographs of pillow basalts from the Dinaridic ophiolitic mélanges. For details see text. Cpx- clinopyroxene; Ab- albite; Pl- plagioclase; Chl- chlorite; Cal- calcite.

Plagioclase is readily replaced by albite, sericite and analcime, so the primary plagioclase chemistry remains unknown. Clinopyroxene is partially replaced by chlorite or actinolite.

Group 5: Vesicular oligophyric to aphyric basalts (Figs. 2f and 3f). Primary assemblage includes labradorite (An_{51-64}), clinopyroxene, Ti-magnetite (21.4-24.41 wt.% TiO_2) and spinel ($Mg_{0.6}Fe_{0.4}Al_{0.8-0.9}Fe_{0.1-0.2}Cr_{1.0}O_4$). High chromium and magnesium content (Mg# = 60.8-63.9, Cr# = 0.53-0.57), accompanied by low titanium (TiO_2 = 0.62-0.67 wt. %) are characteristic for supra-subduction zone type oceanic crust.

Clinopyroxene chemistry

Representative clinopyroxene compositions are shown in Table 2 and plotted in the classification diagram (Morimoto, 1988; Fig. 4). The clinopyroxene from group 1 basalts is preserved only as chemically homogeneous groundmass grain with a diopside composition ($Wo_{45-50}En_{27-39}Fs_{15-25}$). High contents of other-than-quadrilateral components (TiO_2 = 2.71-4.61 wt.%; Al_2O_3 = 7.12-9.56 wt.%) are characteristic of non-orogenetic alkali nature of the host rock (Leterrier et al., 1982). In addition, the analyzed clinopyroxene has high Ti/Al ratio (0.21-0.41) and Mg# (59.0-76.2). Group 2 clinopyroxene is homogeneous augite and subordinate diopside ($Wo_{37-45}En_{34-49}Fs_{15-22}$). The Ti/Al ratio is 0.13-0.20 and Mg# = 60.7-77.6. In the group 3 clinopyroxene is homogeneous or shows reverse and oscillatory zoning. Homogeneous grains have augite-diopside composition ($Wo_{43-48}En_{35-43}Fs_{11-21}$) with medium other-than-quadrilateral components (TiO_2 = 1.03-1.92 wt.%, Al_2O_3 = 2.08-6.49 wt.%). Grains with reverse and oscillatory zoning have augite compositions with low Ti and Al abundances (TiO_2 = 0.2-0.32 wt.%, Al_2O_3 = 1.98-2.29 wt.%). Clinopyroxene from group 4 basalts is augite and only sporadically diopside ($Wo_{38-47}En_{36-50}Fs_{11-25}$) with low other-than-quadrilateral components (TiO_2 = 0.44-2.05 wt.%, Al_2O_3 = 1.74-6.73 wt.%). The Ti/Al ratio is 0.06-0.40, and Mg# is high (Mg# = 63.4-87.8). These geochemical characteristics are typical for extrusive rocks of supra-subduction geotectonic setting.

Chemical composition of clinopyroxene in basalts is used to infer tectonic position of magmas from which they crystallize (Beccaluva et al, 1989). Clinopyroxene from group 2 cannot be used in this way because it crystallized from andesitic magma (Table 3). In the triangular diagram displayed in Fig. 5a, clinopyroxene from group 1 basalts plots in the upper portion of the within-plate basalt field having a maximal TiO_2 content. Clinopyroxene from the group 3 basalts is projected in the overlapping MORB-within-plate basalt field. Clinopyroxene from group 4 and 5 basalts spreads across IAT-MORB array (Fig. 5b).

BULK-ROCK CHEMISTRY

Chemical compositions of analyzed rocks are shown in Table 3. High LOI (up to 8.5 wt.%) corroborates hydrothermal alteration determined by petrographic analysis. The relative mobility of chosen elements was tested by plotting their concentrations against immobile Zr as differentiation index (Fig. 6). Large ion lithophile elements (LILE - Cs, Rb, K, Ba, Sr) show variable and selective mobilization as displayed in Ba - Zr plot (Fig. 6a). High field strength elements (HFSE - Th, Nb, Ta, Ti, Hf, P, Y) and rare earth elements (REE) remained immobile (Fig. 6b-f). Transitional metals (V, Cr, Mn, Fe, Ni, Zn) retained magmatic abundances (Fig. 6g - h). For these reasons, diagram of Winchester and Floyd (1977) based on the immobile elements ratios has been used to classify the rocks (Fig. 7). The analyzed rocks are separated in the field of alkaline and subalkaline basalts to andesite/basalts (Fig. 7). They show similar Zr/TiO_2 ratio (0.004-0.010) and a wide range of Nb/Y ratio, with Nb/Y > 1.25 for alkaline basalts and Nb/Y < 0.47 for subalkaline basalts and andesite/basalts.

Group 1 is represented by four samples (Table 3). This group has clear alkaline nature with high Nb/Y ratio (1.25-1.42), and consists of primitive to slightly evolved basalts (Mg# = 72.5-60.3). It is characterized by significant Th and Nb enrichment (Fig. 8), high Zr/Y ratio (5.34-6.26), very low Zr/Nb and low Ti/Zr ratios (4.1-4.4 and 3.6-8.9, respectively). The TiO_2 (1.71-2.02 wt.%) content and Ti/V ratio (40.2 to 48.4) are atypically low for alkaline basalts (Table 3). The N-MORB normalized abundance plots of immobile trace elements in spider diagrams (Fig. 9a) are characterized by generally smooth and decreasing pattern from Th to Y, with slight HFSE enrichment [e.g. $(Nb/La)_n$ = 1.67-1.99)]. The chondrite normalized REE abundance patterns (Fig. 9b) depict an LREE enrichment with respect to HREE [$(Ce/Lu)_{cn}$ = 4.16-5.94]. The slight Eu anomaly (Eu/Eu^* = 0.94-1.02) points to the crystallization from unfractionated magma. Group 1 basalts plot in the field of continental rift basalts (Fig. 10) in discrimination diagram of Agrawal et al. (2008). This is in accordance with their position in the Th-Hf/3-Nb/16 discrimination diagram where they plot in the WPB field (Fig. 11). The overall geochemical characteristics point to within-plate alkaline basalts.

Group 2 comprises two samples (Table 3), crystallized from evolved magma (Mg# = 43.40-41.67; SiO_2 = 58.47-62.15 wt.%). Low Nb/Y ratio (0.29-0.30) points to subalkaline affinity. These rocks have moderate TiO_2 content (0.80-0.91 wt.%), accompanied by low Ti/V ratio (29.42-29.48). Spider diagrams are characterized by positive anomalies of Th, U, K, La, Ce and marked Nb, Ta, Sr and Ti negative anomalies (Fig. 9c). The LREE display enrichment relative to the HREE [$(Ce/Lu)_{cn}$ = 3.38-3.55] (Fig. 9d). These rocks plot in the field of calc-alkaline basalts in the Nb_N-Th_N (Fig. 8) and Th-Hf/3-Nb/16 discrimination diagrams (Fig. 11), respectively. This is in accordance with their overall geochemical characteristics.

Group 3 basalts are represented by seven samples (Table 3). These rocks are subalkaline, as evidenced by their Nb/Y ratio (0.13-0.47). The Mg# (71.5-51.43) indicate a crystallization from both primitive and evolved magmas. The TiO_2 ranges from 1.23 to 2.20 wt.%, with the same trend of the Ti/V ratio (from 33.85 to 45.96). These rocks display enrichment in Th and Nb and plot in the E-MORB field (Fig. 8). Spider diagrams (Fig. 9e) are characterized by variation in both LILE and HFSE contents [$(Nb/La)_n$ = 0.68-2.10)]. The LREE display slight enrichment relative to the HREE [$(Ce/Lu)_{cn}$ = 1.45-1.78)] (Fig. 9f). Most of the samples plot in the CRB field in discrimination diagram of Agrawal et al. (2008, Fig 10). In summary, the overall geochemical characteristics of this group indicate E-MORB affinity.

Group 4 comprises five samples (Table 3), with clear sub-alkaline nature (Nb/Y = 0.04-0.10). Wide range of the Mg# (70.1-37.0) points to crystallization from primitive to evolved magmas. The Ti/V ratio is ranging from 17.1 to 34.71, while the TiO_2 content is low (0.71-0.95 wt.%). The incompatible elements abundance patterns in spider diagram (Fig. 9g) are characterized by depletion of LILE and HFSE,

Table 2 - Selected microprobe analyses and structural formulae of clinopyroxenes from pillow basalts from the ophiolitic mélange of Dinarides.

	zmtd-4	doz-13	doz-13	doz-9b	doz-9b	doz-6c	doz-6c	wvz-3a	wvz-3a	wvz-4a	zmtd-2	zmtd-2	doz-3a	doz-3a	dub-2	dub-2	wvz-2a	wvz-2a
Analysis	4	3	4	3	7	8	9	3	4	2	1	2	3	4	18	20	13	28
Position	c	c	c	c	c	c	r	c	c	c	c	r	c	c	c	r	c	c
Group	1	1	1	2	2	3	3	3	3	3	4	4	4	4	5	5	5	5
SiO_2	43.52	44.79	43.68	47.95	47.37	50.06	50.13	44.65	43.86	46.83	53.63	53.83	48.32	50.55	51.84	49.57	48.67	47.38
TiO_2	3.80	3.40	4.61	1.65	1.88	1.12	1.54	2.11	1.86	2.32	0.32	0.23	1.11	1.25	0.68	1.33	1.52	2.05
Al_2O_3	8.80	8.07	7.12	6.42	6.10	4.04	2.73	10.65	12.61	7.41	2.29	2.04	6.62	2.38	1.64	2.13	5.00	5.21
Cr_2O_3	0.09	0.17	0.09	0.05	0.08	0.24	0.02	0.09	0.11	0.12	0.24	0.41	0.27	0.06	0.01	0.00	0.17	0.24
Fe_2O_3	3.70	2.17	3.37	0.52	1.21	0.51	1.17	0.89	2.56	1.35	0.00	0.00	3.78	1.75	2.05	2.69	1.67	2.23
FeO	8.65	9.15	10.68	8.17	9.36	7.06	10.58	11.75	8.20	11.03	5.10	4.96	4.44	9.16	7.33	12.09	8.78	8.70
MnO	0.19	0.26	0.28	0.22	0.29	0.10	0.33	0.28	0.15	0.32	0.14	0.11	0.16	0.21	0.32	0.38	0.27	0.21
MgO	10.48	11.26	8.62	13.52	12.03	14.12	12.65	12.34	11.52	12.96	18.48	19.13	14.38	13.67	16.49	12.53	13.08	12.32
CaO	19.88	19.72	20.86	19.22	18.78	20.82	19.85	15.44	17.08	16.04	19.02	19.00	21.32	20.66	18.83	18.35	20.29	20.49
Na_2O	0.51	0.38	0.71	0.34	0.64	0.40	0.52	0.26	0.35	0.64	0.17	0.18	0.25	0.29	0.30	0.46	0.26	0.29
Total	99.66	99.40	100.02	98.09	97.81	98.47	99.53	98.56	98.86	99.07	99.37	99.90	100.67	99.96	99.50	99.54	99.71	99.12
Si	1.66	1.70	1.68	1.82	1.81	1.88	1.90	1.70	1.66	1.77	1.96	1.95	1.78	1.90	1.93	1.89	1.83	1.80
Al^{IV}	0.34	0.30	0.32	0.18	0.19	0.12	0.10	0.30	0.34	0.23	0.04	0.05	0.22	0.10	0.07	0.10	0.17	0.20
Al^{VI}	0.05	0.06	0.00	0.10	0.09	0.06	0.02	0.18	0.22	0.10	0.05	0.04	0.07	0.00	0.00	0.00	0.05	0.03
Ti	0.11	0.10	0.13	0.05	0.05	0.03	0.04	0.06	0.05	0.07	0.01	0.01	0.03	0.04	0.02	0.04	0.04	0.06
Cr	0.00	0.01	0.00	0.00	0.00	0.01	0.00	0.00	0.00	0.00	0.01	0.01	0.01	0.00	0.00	0.00	0.00	0.01
Fe^{3+}	0.11	0.06	0.10	0.01	0.03	0.01	0.03	0.03	0.07	0.04	0.00	0.00	0.10	0.05	0.06	0.08	0.05	0.06
Fe^{2+}	0.28	0.29	0.34	0.26	0.30	0.22	0.33	0.37	0.26	0.35	0.16	0.15	0.14	0.29	0.23	0.39	0.28	0.28
Mn	0.01	0.01	0.01	0.01	0.01	0.00	0.01	0.01	0.00	0.01	0.00	0.00	0.00	0.01	0.01	0.01	0.01	0.01
Mg	0.60	0.64	0.49	0.76	0.69	0.79	0.71	0.70	0.65	0.73	1.00	1.03	0.79	0.76	0.91	0.71	0.73	0.70
Ca	0.81	0.80	0.86	0.78	0.77	0.84	0.81	0.63	0.69	0.65	0.74	0.74	0.84	0.83	0.75	0.75	0.82	0.83
Na	0.04	0.03	0.05	0.03	0.05	0.03	0.04	0.02	0.03	0.05	0.01	0.01	0.02	0.02	0.02	0.03	0.02	0.02
Total	4.00	4.00	4.00	4.00	4.00	4.00	4.00	4.00	4.00	4.00	3.99	4.00	4.00	4.00	4.00	4.00	4.00	4.00
Mg#	68.37	68.67	59.00	74.69	69.61	78.08	68.07	65.18	71.48	67.69	86.60	87.30	85.23	72.68	80.03	64.88	72.63	71.62
Wo	45.22	44.56	47.66	42.76	42.77	44.86	42.42	36.23	41.22	36.55	38.95	38.32	44.82	42.85	38.29	38.70	43.42	44.40
En	33.17	35.40	27.40	41.85	38.13	42.32	37.61	40.27	38.71	41.10	52.68	53.69	42.06	39.45	46.64	36.78	38.94	37.14
Fs	21.61	20.04	24.95	15.38	19.10	12.82	19.97	23.50	20.07	22.35	8.37	7.99	13.13	17.71	15.07	24.52	17.65	18.46

Formula calculated on the basis of 6 oxygen and 4 cations. $^{+}$). c- core of the clinopyroxene grain; r- rim of the clinopyroxene grain; Mg# = 100*Mg/(Mg + Fe^{2+}). Wo = 100*Ca/(Ca + Mg + Mn + Fe^{2+} + Fe^{3+}), En = 100*Mg/(Ca + Mg + Mn + Fe^{2+} + Fe^{3+}) i Fs = 100*(Mn + Fe^{2+} + Fe^{3+})/(Ca + Mg + Mn + Fe^{2+} + Fe^{3}).

Table 3 - Chemical analyses of the pillow basalts from the ophiolitic mélange of Dinarides.

Sample	zmtd-03	zmtd-04	doz-13	doz-04a	doz-9a	doz-9b	doz-6b	doz-6c	doz-6d	wvz-3	wvz-4a	zmtd-1a	zmtd-1b	zmtd-1c	zmtd-2	doz-3A	doz-11b	dub-2	wvz-2
Group	1				2		3					4					5		
Location	MOM	MOM	BOM	ZOM	KKOM	KKOM	KKOM	KKOM	KKOM	MaOM	MaOM	KOM	KOM	KOM	KOM	ZOM	KKOC	KKOC	KoOM
SiO_2	39.10	50.28	54.75	53.67	62.15	58.47	47.46	47.78	47.38	42.31	50.70	46.64	47.18	47.46	53.46	48.26	43.28	45.14	48.93
TiO_2	2.02	1.91	1.71	1.79	0.80	0.91	1.17	1.19	1.23	2.20	1.88	0.84	0.90	0.88	0.71	0.95	1.63	0.97	0.95
Al_2O_3	16.07	16.78	16.60	15.47	15.35	15.95	16.47	16.61	15.85	16.54	14.90	18.82	18.90	18.57	13.43	18.73	19.59	14.24	15.87
FeO_{tot}	11.82	7.88	6.09	6.54	6.16	7.39	7.37	7.47	7.58	9.86	9.32	10.81	10.16	9.88	7.57	6.71	11.90	10.76	7.70
MnO	0.19	0.11	0.09	0.10	0.04	0.04	0.21	0.20	0.21	0.18	0.16	0.14	0.14	0.16	0.16	0.10	0.47	0.21	0.16
MgO	12.58	6.70	4.67	8.71	2.22	2.86	9.35	9.39	9.67	9.01	4.98	3.20	3.22	4.23	8.92	5.43	8.44	13.98	8.89
CaO	4.44	5.38	6.52	2.08	4.13	3.27	5.81	5.87	5.42	10.75	8.47	8.95	8.66	7.67	7.14	9.18	2.99	5.58	7.14
Na_2O	0.36	4.12	4.53	5.07	5.33	7.11	5.23	4.97	5.45	0.32	5.03	5.08	5.09	5.27	3.11	3.81	3.37	2.41	3.81
K_2O	3.15	1.23	1.14	0.12	0.97	0.65	0.10	0.18	0.08	1.84	0.12	<0.04	<0.04	<0.04	1.60	0.61	0.59	0.08	0.50
P_2O_5	0.31	0.38	0.32	0.40	0.32	0.33	0.15	0.14	0.15	0.19	0.25	0.14	0.12	0.10	0.09	0.08	0.16	0.11	0.13
LOI	8.50	4.20	2.80	5.10	1.80	2.00	5.80	5.40	6.10	5.60	3.10	4.10	4.30	4.50	2.80	5.20	6.00	5.20	5.00
Total	99.85	99.84	99.90	99.78	99.95	99.80	99.94	99.95	99.96	99.89	99.94	99.92	99.80	99.82	99.83	99.81	99.74	99.87	99.93
Mg#	67.8	62.8	60.3	72.5	41.7	43.4	71.5	71.5	71.7	64.4	51.4	37.0	38.6	45.9	70.0	61.6	58.4	72.0	69.6
Cs	4.9	2.7	1.5	3.0	0.2	0.1	4.3	3.5	4.7	7.3	1.0	0.1	0.1	<0,1	2.7	1.1	7.9	<0.1	0.9
Rb	85.2	21.9	18.5	2.9	12.0	7.0	1.9	3.2	1.3	42.3	2.4	<0.5	<0.5	<0.5	23.3	6.3	20.0	1.1	12.8
Ba	708.7	345.6	280.5	73.3	73.6	56.3	61.6	80.1	37.5	121.1	85.2	10.3	10.9	6.5	143.6	28.2	212.8	25.8	59.9
Th	3.2	2.9	2.9	3.2	2.2	2.3	0.5	0.4	0.6	1.2	0.5	<0.1	<0.1	<0.1	0.3	<0.1	<0.1	0.3	0.7
U	0.9	1.0	0.9	0.9	0.6	1.0	0.1	0.1	0.1	0.3	0.4	0.1	0.1	0.1	0.1	0.2	0.3	0.1	0.2
Ta	2.0	2.1	1.9	2.0	0.5	0.5	0.2	0.2	0.1	0.8	0.5	0.1	0.1	0.1	0.1	0.1	0.1	0.1	0.1
Nb	32.8	33.9	30.1	33.1	7.0	8.0	2.9	3.2	3.0	13.7	7.0	1.1	1.1	1.0	1.9	0.7	1.2	1.4	1.5
Sr	47.9	525.2	393.6	284.9	186.5	155.4	183.4	246.0	135.0	45.6	142.7	136.9	93.6	68.6	71.7	350.5	88.5	106.1	114.5
Zr	136.5	139.9	128.8	145.9	80.1	94.2	89.9	92.7	88.3	151.0	126.0	52.3	53.7	54.6	33.1	56.3	81.2	82.8	68.5
Hf	3.1	3.7	3.5	3.6	2.3	3.0	2.2	2.7	2.5	4.0	3.5	1.4	1.6	1.5	1.3	1.6	2.6	2.4	1.9
Y	25.4	25.5	24.1	23.3	24.3	26.6	22.3	23.2	22.3	28.9	41.3	23.2	21.4	21.3	19.4	20.0	27.5	28.4	21.5
Cr	287.4	273.7	232.6	301.0	294.2	348.9	280.5	273.7	280.5	499.5	314.7	294.2	307.9	301.0	191.6	307.9	328.4	222.1	437.9
Ni	199.0	239.0	167.0	196.0	120.0	172.0	104.0	109.0	100.0	226.0	72.0	138.0	172.0	170.0	103.0	65.0	100.0	144.1	166.0
Sc	30.0	30.0	28.0	21.0	19.0	23.0	30.0	30.0	31.0	43.0	36.0	39.0	41.0	41.0	35.0	33.0	41.0	32.0	32.0
V	250.0	266.0	255.0	224.0	163.0	185.0	207.0	208.0	208.0	287.0	308.0	183.0	219.0	152.0	249.0	230.0	295.0	268.0	254.0
La	17.7	21.8	19.0	21.2	9.6	12.6	4.5	4.6	4.7	7.0	7.3	2.0	4.5	1.3	3.0	1.9	8.2	4.7	3.0
Ce	37.1	44.7	41.2	44.4	23.1	26.1	11.1	11.9	11.8	20.2	19.6	4.4	4.7	3.3	5.0	6.3	14.3	12.3	10.1
Pr	4.8	5.4	4.9	5.2	3.4	3.7	1.8	1.9	1.8	2.7	3.1	0.9	0.9	0.7	1.0	1.1	2.8	2.0	1.6
Nd	20.4	23.5	21.6	21.6	16.0	16.1	9.0	9.6	9.2	12.4	16.5	5.1	4.7	3.6	5.4	6.4	14.4	9.7	8.2
Sm	4.4	4.5	4.0	4.1	4.1	3.9	2.6	2.8	2.5	3.6	4.4	1.8	1.7	1.5	1.8	2.2	3.4	3.4	2.4
Eu	1.6	1.5	1.4	1.4	1.3	1.3	1.0	1.1	1.0	1.4	1.7	0.8	0.7	0.6	0.7	0.8	1.1	1.2	0.9
Gd	4.4	4.8	4.4	4.2	4.3	4.3	3.3	3.4	3.4	4.6	6.0	2.7	2.6	2.4	2.5	2.8	4.1	4.6	3.1
Tb	0.9	0.9	0.9	0.8	0.9	0.8	0.7	0.7	0.7	1.0	1.2	0.6	0.6	0.6	0.6	0.6	0.8	0.8	0.7
Dy	4.8	4.6	4.6	4.0	4.5	4.4	3.9	4.3	4.0	5.5	7.3	3.6	3.9	3.4	3.3	3.6	4.5	4.9	4.0
Ho	0.9	0.9	0.8	0.8	0.8	0.8	0.8	0.8	0.8	1.1	1.4	0.7	0.8	0.8	0.7	0.7	1.0	1.0	0.8
Er	2.6	2.7	2.5	2.4	2.3	2.5	2.3	2.4	2.3	3.1	4.4	2.4	2.4	2.3	2.2	2.2	2.9	3.1	2.3
Tm	0.4	0.4	0.4	0.4	0.3	0.4	0.4	0.4	0.3	0.5	0.6	0.3	0.4	0.4	0.3	0.3	0.5	0.5	0.3
Yb	2.6	2.3	2.2	2.2	1.9	2.1	2.1	2.3	2.1	3.0	3.9	2.1	2.2	2.2	1.9	2.0	2.7	2.9	2.1
Lu	0.4	0.3	0.3	0.3	0.3	0.3	0.3	0.3	0.3	0.5	0.6	0.3	0.4	0.4	0.3	0.3	0.4	0.5	0.3

Oxides in wt.%, trace elements in ppm. Mg# = 100*MgO/(MgO + 0.9*FeO_{total}). LOI- loss on ignition.
MOM- Medvednica ophiolitic mélange; BOM-Banija ophiolitic mélange; ZvOM- Zvornik ophiolitic mélange; KKOM- Krivaja-Konjuh ophiolitic mélange; KKOC- Krivaja-Konjuh ophiolitic complex; MaOM- Maljen ophiolitic mélange; KOM- Kalnik ophiolitic mélange; ZOM- Zlatibor ophiolitic mélange; KoOM- Kopaonik ophiolitic mélange.

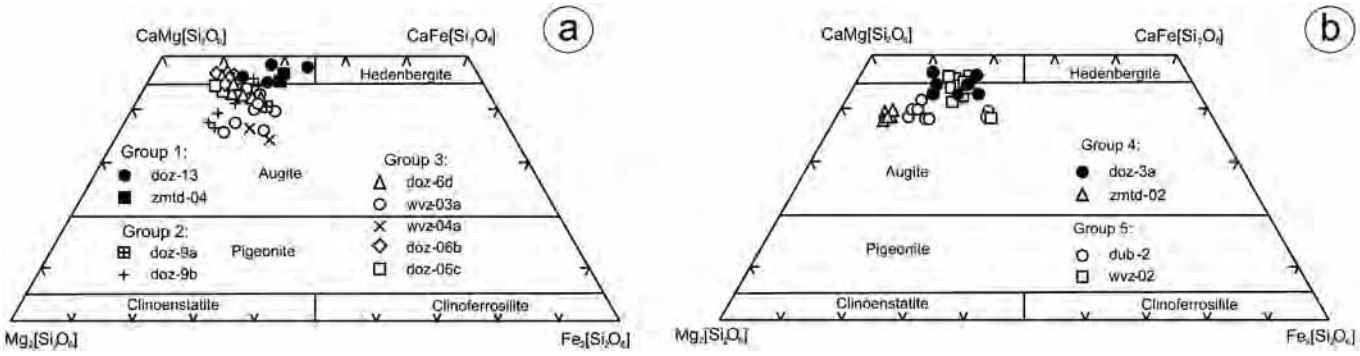

Fig. 4 - Plots of clinopyroxene compositions in the En-Wo-Fs ($Mg_2Si_2O_6$-$Ca_2Si_2O_6$-$Fe_2Si_2O_6$) diagram with the nomenclature fields of Morimoto (1988) for: (a) group 1, 2 and 3 basalts; (b) group 4 and 5 basalts.

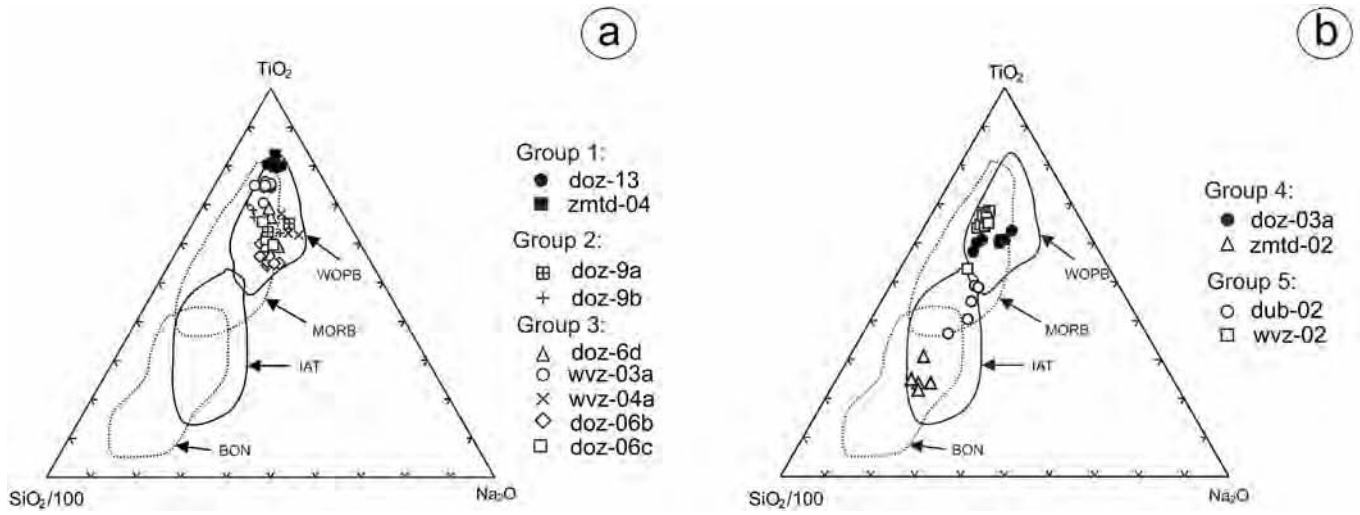

Fig. 5 - Discrimination diagram SiO_2/100 - Na_2O - TiO_2 (simplifed after Beccaluva et al., 1989) for clinopyroxene from the basalts from oceanic units of Dinarides. MORB- mid-ocean ridge basalts; IAT- island-arc tholeiites; BON- boninite; WOPB- within ocean plate basalts for: (a) group 1, 2 and 3 basalts; (b) group 4 and 5 basalts.

with slight Nb-Ta negative anomaly [$(Nb/La)_n$ = 0.26-0.83)]. The REE abundance pattern (Fig. 9h) has convex shape, depleted in LREE relative to MREE [$(Ce/Sm)_{cn}$ = 0.55-0.72] and HREE [$(Ce/Lu)_{cn}$ = 0.40-0.93]. The overall geochemical characteristics point to IAT affinity of group 4 basalts.

Group 5 is represented by three samples (Table 3) displaying sub-alkaline affinity (Nb/Y= 0.04-0.07). These rocks crystallized from relatively primitive magmas (Mg# =7 2.0-58.4). Concentration of the TiO_2 is moderate to high (0.95-1.63 wt.%) and samples are characterized by elevated Ti/V ratio (21.7-33.1). The Nb is very low (Table 3) and consequently Zr/Nb ratio is high (45.8-67.7), otherwise typical for N-MOR basalts. Th is enriched relative to Nb, besides sample doz-11b having low Th content (Fig 8). The incompatible element abundance patterns in spider diagram (Fig. 9i) display both LILE enrichment and depletion as well as HFSE depletion, with distinct Ta-Nb trough [$(Nb/La)_n$ = 0.16-0.53)], indicating supra-subduction influence. REE abundance patterns (Fig. 9j) are generally flat to moderately convex [$(Ce/Sm)_{cn}$ = 0.90-1.05, $(Ce/Lu)_{cn}$ = 1.09-1.50], and display REE enrichment 9-10 times relative to chondrite, similar to E-MORB. On the basis of geochemical characteristics, group 5 are tentatively classified as BABB.

RADIOLARIAN DATING

A single chert sample from the Krivaja-Konjuh ophiolite mélange (doz-10) yielded poorly preserved but identifiable radiolarians. The sample was treated with diluted (5%) hydrofluoric acid.

The genera designations follow the revision of O'Dogherty et al. (2009 and 2017). The zonation proposed by Baumgartner et al. (1995) and based on Unitary Associations was used to date the assemblage. The identified radiolarians are illustrated in Plate 1.

Radiolarians are characteristic of the Middle Jurassic age. Presence of *Eucyrtidiellum pustulatum* Baumgartner (UAZ 5-7 of Baumgartner et al., 1995) and *Striatojaponocapsa conexa* (Matsuoka) (UAZ 4-7 of Baumgartner et al., 1995) indicate a late Bajocian-early Bathonian to late Bathonian-early Callovian age (UAZ 5-7).

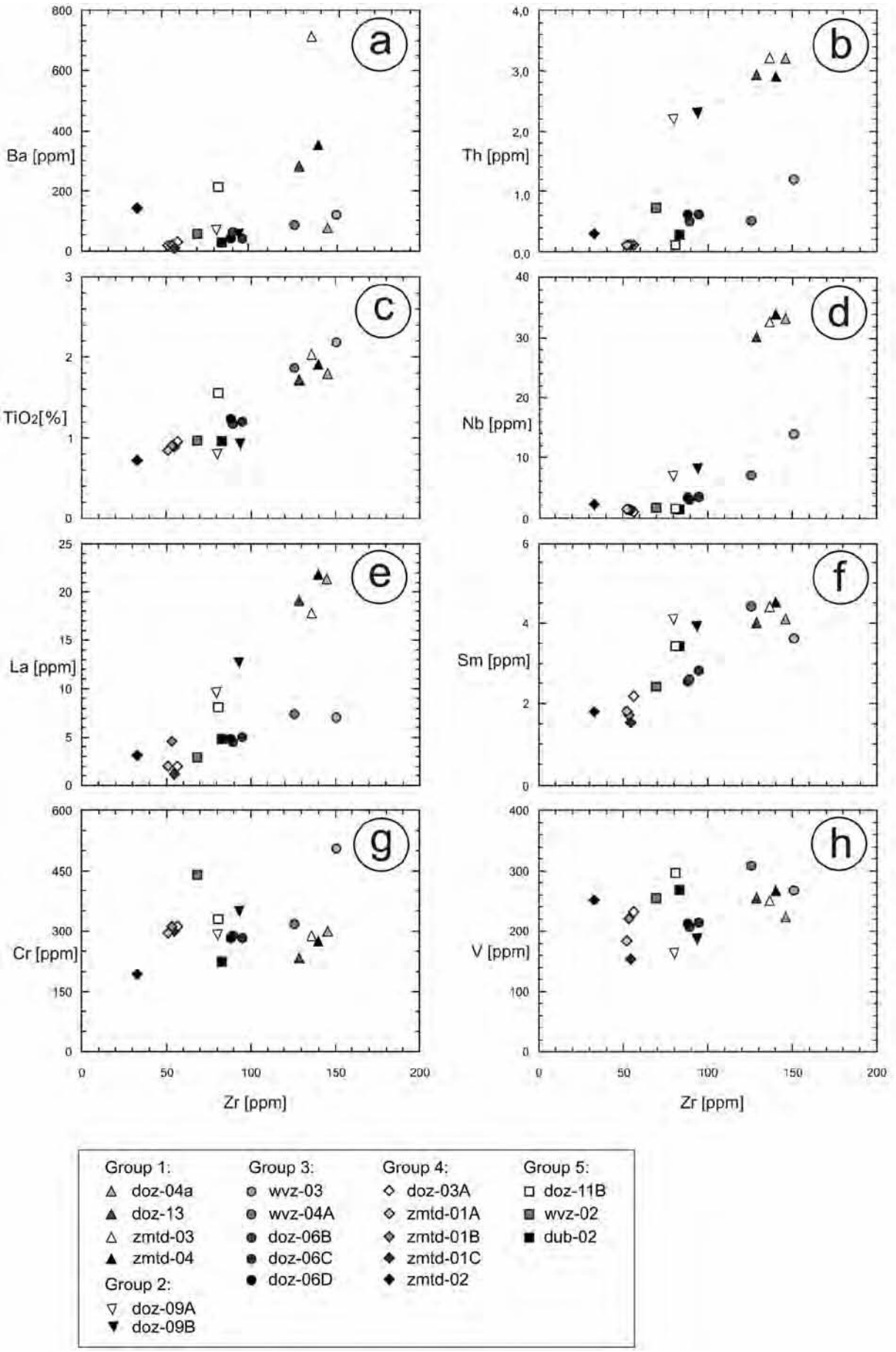

Fig. 6 - Variation diagrams for selected elements vs. Zr, here assumed as fractionation index for the basalts from the Dinaridic ophiolitic mélanges.

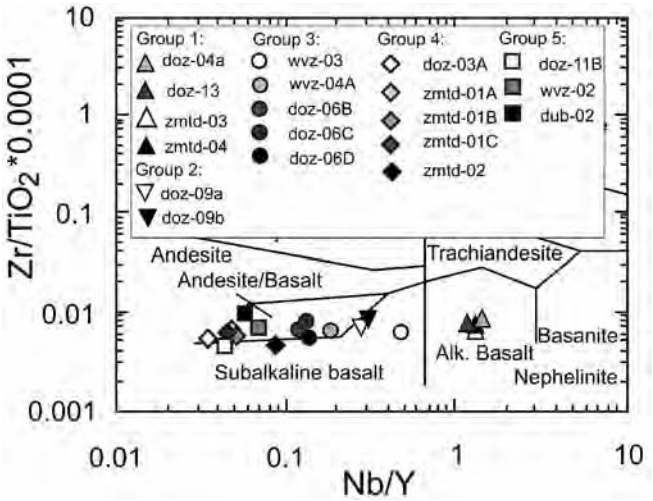

Fig. 7 - Nb/Y - Zr/TiO_2*0.001 classification diagram (Winchester and Floyd, 1977) for the basalts from the oceanic units of Dinarides.

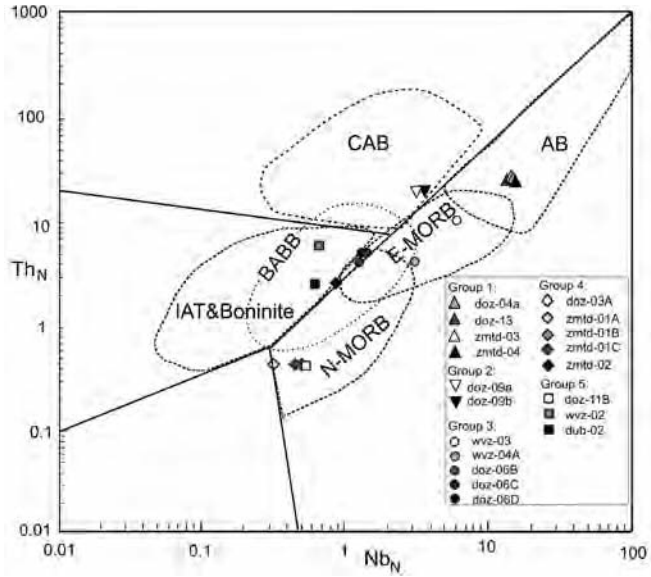

Fig. 8 - N-MORB normalized Nb_N - Th_N discrimination diagram (Saccani, 2015). Normalization values are from Sun and McDonough (1989).

According to Baumgartner et al. (1995) *Zhamoidellum ventricosum* Dumitrica first occurs in UAZ 8, however this taxon has already been found in older assemblages (UAZ 6 in Chiari et al., 2013; UAZ 6-7 in Šmuc and Goričan, 2005 and O'Dogherty et al., 2006). Moreover, *Transhsuum crassum* Chiari, Marcucci and Prela has its first occurrence in UAZ 6 (Chiari et al., 2002), but because of poor preservation we prefer to indicate these specimens as "cf. species" (see Plate 1).

Middle Jurassic (UAZ 5 of Baumgartner et al., 1995) radiolarian assemblage from the chert-shales slide block within the ophiolitic mélange has previously been reported from the Krivaja - Konjuh ophiolitic mélange (Šegvić et al., 2014). Furthermore, radiolarian cherts of Middle Jurassic age are found in mélanges of the neighbouring ophiolitic complexes in Croatia (Halamić et al., 1999) and Serbia (Gawlick et al., 2009). In ophiolite complexes of Albania and Greece Middle Jurassic cherts are found both in direct contact with the basalts as well as blocks within the ophiolitic mélange (e.g. Bortolotti et al., 2013; Šegvić et al., 2014).

DISCUSSION

The studied pillow basalts of the Dinaridic ophiolitic mélange represent rocks of five different tectonomagmatic groups: group 1 (within plate alkali basalts), group 2 (CAB), group 3 (E-MORB), group 4 (IAT) and group 5 (BABB). The geodynamic interpretation of these groups is based on presented results and supported by literature data from Greece and Albania (summarized in Bortolotti et al., 2013) and nothwestern Croatia (Slovenec and Lugović, 2009; Slovenec et al., 2010; 2011). Groups 1 to 3 belong to the initial stage of intracontinetal rifting and oceanic basin opening (Fig. 12a) while groups 4 and 5 belong to the convergence stage affected by subduction zone (Fig. 12b).

In the evolution of the Neotethys, Middle Triassic has been recognized as a period of oceanic basin opening (e.g. Marccuci et al., 1994; Danelian and Robertson, 2001; Gawlick et al., 2008; 2009; Bortolotti et al., 2013). It was characterized by alkaline, calc-alkaline and variably enriched subalkaline magmatism (Pe-Piper, 1998; Saccani et al., 2015). This phenomenon is interpreted by heterogenity of both lithospheric and asthenospheric mantle - CAB magmas were derived by melting of SSZ-type lithospheric mantle (Pe-Piper, 1998; Saccani et al., 2015), alkaline magmas originated from OIB-type metasomatized asthenosphere (Saccani et al., 2015), while subalkaline basalts were derived from primitive asthenospheric mantle, sporadically enriched by OIB-component.

According to literature data, alkaline basalts zmtd-03 and zmtd-04 from Medvednica ophiolitic mélange are late Anisian to early Ladinian (Halamić et al., 1998). Other samples from group 1 could be of similar age and are attributed to the same phase of oceanic evolution, i.e. intracontinental rifting. These rocks are similar to alkaline basalts from ophiolitic mélanges of northwestern Croatia (Slovenec et al., 2010; 2011), as well as those from Albanides and Hellenides (Bortolotti et al., 2013; Fig. 9b), which have the similar ages. Group 2 CAB probably belongs to the same stage of oceanic evolution. Middle Triassic age reported for these rocks (Karamata et al., 2000) is in accordance with this proposition. This group is similar to CAB from ophiolitic mélanges in Albania and Greece (Fig. 9d). Middle Triassic E-MORBs are reported from ophiolitic mélanges of northwestern Croatia (Slovenec et al., 2011). It could be proposed that group 3 E-MORBs presented in this paper belongs to the same time period. These rocks probably represent the initial phase of magmatism at a spreading ridge. They are comparable with similar rocks of ophiolitic mélanges in Albania and Greece (Fig. 8f).

Change from divergent to convergent regime within the Neotethys is generally placed in Early to early Middle Jurassic (e.g. Gawlick et al., 2008; Schmid et al., 2008; Bortolotti et al., 2013) with formation of oceanic lithosphere in supra-subduction setting (e.g. Pamić et al., 2002; Saccani et al., 2011; Bortolotti et al., 2013). Convergent regime was complex with different types of magmatism - N-MORB, IAT, boninitic, BABB, low-K tholeiitc and

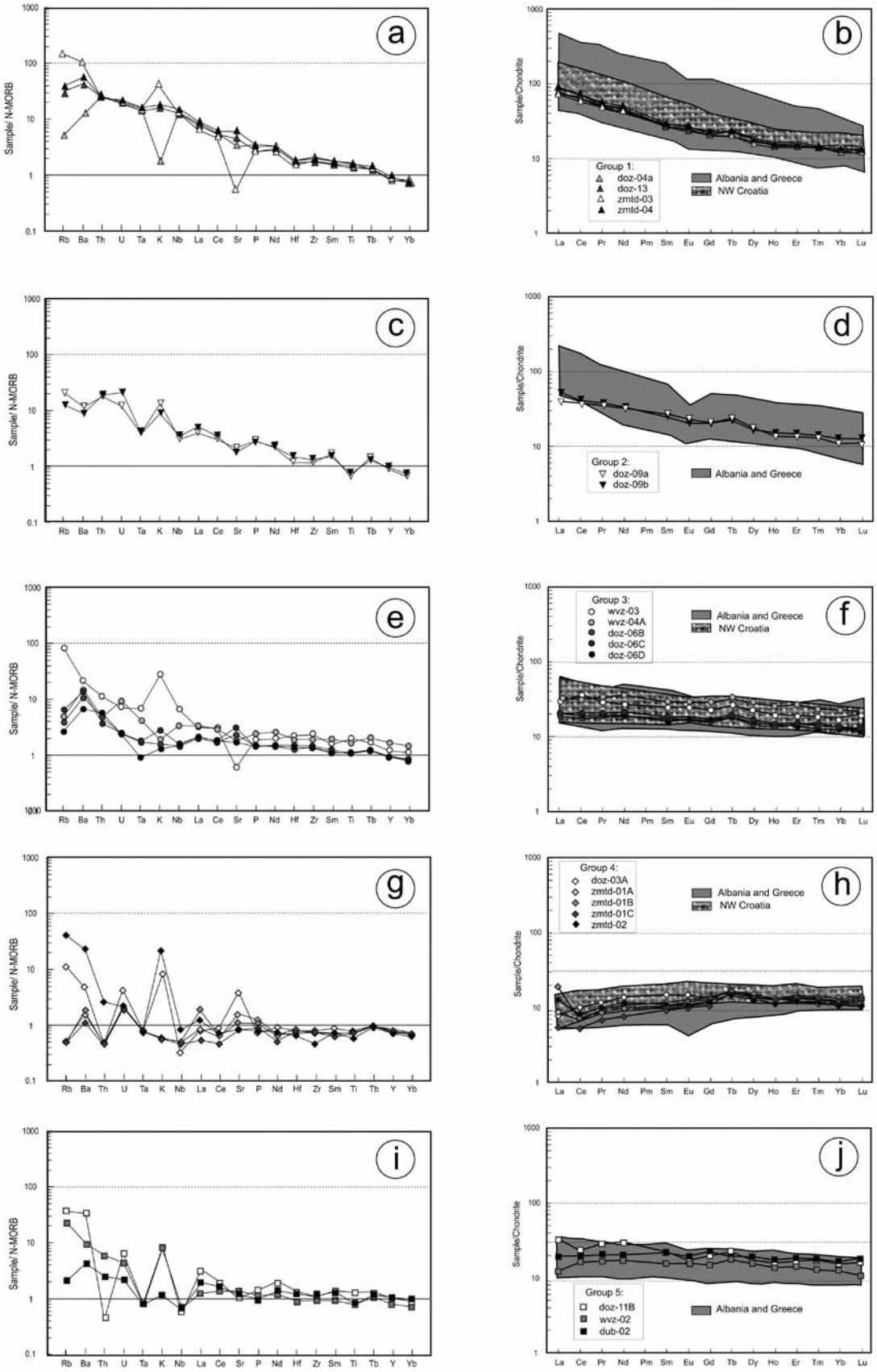

Fig. 9 - Normalized patterns for the basalts from the Dinaridic ophiolitic mélanges. (a) N-MORB-normalized multielement and (b) REE chondrite-normalized patterns for group 1 basalts. (c) N-MORB-normalized multielement and (d) REE chondrite-normalized patterns for group 2 basalts. e) N-MORB-normalized multielement and (f) REE chondrite-normalized patterns for group 3 basalts. (g) N-MORB-normalized multielement (g) and (h) REE chondrite-normalized patterns for group 4 basalts. N-MORB-normalized multielement (i) and REE chondrite-normalized patterns (j) for group 4 basalts. Normalization values are from Sun and McDonough (1989). Fields for Greece and Albania (Bortolotti et al., 2013), and NW Croatia (Slovenec and Lugović, 2009; Slovenec et al., 2010; 2011) are plotted for correlation.

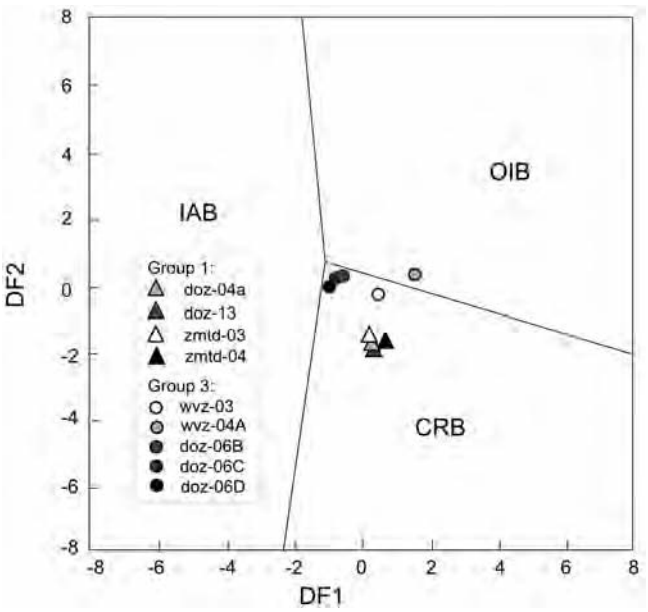

Fig. 10 - DF1 - DF2 diagram (Agrawal et al., 2008; DF1 = 0.5533 loge (La/Th) + 0.2173 loge (Sm/Th) - 0.0969 loge (Yb/Th) + 2.0454 loge (Nb/Th) - 5.6305; DF2 = -2.4498 loge (La/Th) + 4.8562 loge (Sm/Th) - 2.1240 loge (Yb/Th) - 0.1567 loge (Nb/Th) + 0.94) for the alkali basalts from ophiolitic mélanges of Dinarides. IAB- island-arc basalts; OIB- ocean-island basalts; CRB- continental rift basalts.

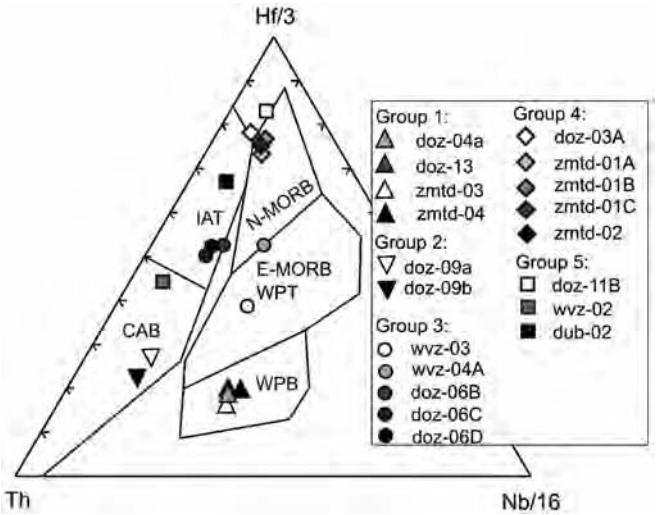

Fig. 11 - Th - Nb/16 - Hf/3 discrimination diagram (Wood, 1980). N-MORB- normal mid-ocean ridge basalts; E-MORB- enriched MORB, WPT- within-plate tholeiites; WPB-within-plate basalts; CAB- calc-alkali basalts; IAT- island-arc tholeiites.

CAB, evolving through time and space (Bortolotti et al., 2013; Saccani et al., 2017). Group 4 basalts showing IAT characteristics probably developed in an intra-oceanic arc settings. Similar rocks of Middle to Late Jurassic age are reported from northwestern Croatia (Slovenec et al., 2011), Greece and Albania (summarized in Bortolotti et al., 2013; Fig. 9h). Sample dub-02 (Krivaja-Konjuh ophiolitic complex) from group 5 is biostratigraphically dated as Middle Jurassic. The group 5 is tentatively determined as BABB due to enriched REE pattern accompanied by Nb-Ta depletion. If the presumption is correct, this could be the first report of Middle Jurassic BABB crust in the Western Vardar Ophiolitic Unit. Group 5 is comparable to BABB from the ophiolites of Hellenides (Fig. 9j).

CONCLUSIONS

In this paper new geochemical and biostratigraphical data on pillow basalts and related pelagic sediments, covering the area from nothwestern Croatia to southern Serbia are presented. Basalts are divided into five tectonomagmatic groups: WPAB, CAB, E-MORB, IAT and BABB. Radiolarites associated with basalt from BABB group are dated as Middle Jurassic (late Bajocian to early Callovian).

Middle Triassic terminal phase of intracontinental rifting was characterized by effusion of coeval basalts having different geochemical characteristics - CAB, WPAB and E-MORB. This was a consequence of mantle heterogenities, rather than different geodynamic processes.

Middle Jurassic oceanic crust developed under the supra-subduction influence in the compressional tectonic regime. In this paper, two types of magmatism related to this phase are recognized - IAT and BABB. Basalts of IAT geochemical affinities developed in an intra-oceanic arc settings, while occurence of basalts with BABB affinity tentatively indicates the possibility of back-arc basin existing in this area during the Middle Jurassic.

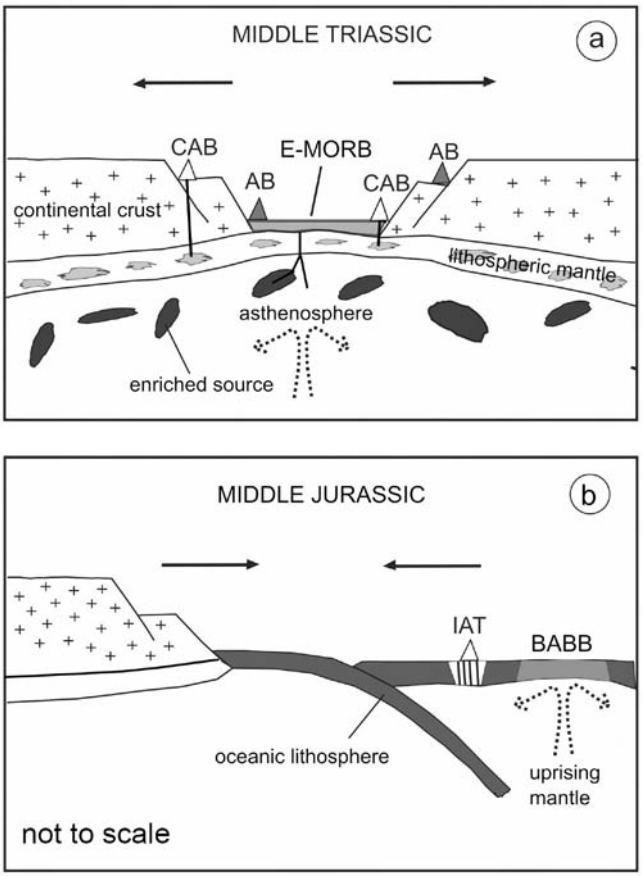

Fig. 12 - Schematic geodynamic model for Dinaridic Neothetys evolution (not to scale): (a) advanced intracontinental rifting stage with contemporaneous alkaline basalt, CAB and E-MORB magmatism; (b) the convergent stage with IAT and BABB magmatism.

ACKNOWLEDGEMENTS

This study is a contribution to the scientific project "Tectonomagmatic correlation of fragmented oceanic lithosphere in the Dinarides" (grant no. 195-1951126-3205) funded by the Croatian Ministry of Science, Education and Sports. We thank to H.-P. Meyer for the microprobe facilities and I. Fin for excellent polished thin sections. Critical comments by B. Šegvić and V. Garašić helped to improve an early version of the manuscript. Constructive and thorough reviews by E. Saccani and M. Chiari, as well as the editiorial processing and suggestions by L. Pandolfi are greatly acknowledged.

REFERENCES

Agrawal S., Guevara M. and Verma S.P., 2008. Tectonic discrimination of basic and ultrabasic volcanic rocks through log-transformed ratios of immobile trace elements. International Geol. Rev., 50: 1057-1079.

Babić Lj., Hochuli P A. and Zupanič J., 2002. The Jurassic ophiolitic mélange in the NE Dinarides: Dating, internal structure and geotectonic implications. Ecl. Geol. Helv., 95: 263-275.

Baumgartner P.O., Bartolini A., Carter E.S., Conti M., Cortese G., Danelian T., De Wever P., Dumitrica P., Dumitrica-Jud R., Goričan Š., Guex J., Hull D.M., Kito N., Marcucci M., Matsuoka A., Murchey B., O'Dogherty L., Savary J., Vishnevskaya V., Widz D. and Yao, A., 1995. Middle Jurassic to Early Cretaceous radiolarian biochronology of Tethys based on Unitary Associations. In P.O. Baumgartner, L. O'Dogherty, Š. Goričan, E. Urquhart, A. Pillevuit and P. De Wever (Eds.) Middle Jurassic to Lower Cretaceous Radiolaria of Tethys: Occurrences, systematics, biochronology. Mém. Géol. Lausanne, 23: 1013-1038.

Beccaluva L., Macciota G., Piccardo G.B. and Zeda O., 1989. Clinopyroxene composition of ophiolite basalts as petrogenetic indicator. Chem. Geol,. 77: 165-182.

Bernoulli D. and Laubscher H., 1972. The palinspastic problem of the Hellenides. Ecl. Geol. Helv., 65: 107-118.

Bortolotti,V. and Principi G. 2005. Tethyan ophiolites and Pangea break-up. Isl. Arc, 14: 442-470.

Bortolotti V., Carras N., Chiari M., Fazzuoli M., Nirta G., Principi G. and Saccani E., 2009. The ophiolite-bearing mélange in the early Tertiary Pindos flysch of Etolia (Central Greece). Ofioliti, 34: 83-94.

Bortolotti V., Chiari M., Marcucci M., Marroni M., Pandolfi L., Principi G. and Saccani E., 2004. Comparison among the Albanian and Greek Ophiolites: in search of constraints for the evolution of the Mesozoic Tethys Ocean. Ofioliti, 29: 19-35.

Bortolotti V., Chiari M., Marroni M., Pandolfi L., Principi G. and Saccani E., 2013. Geodynamic evolution of ophiolites from Albania and Greece (Dinaric-Hellenic belt): one, two, or more oceanic basins? Intern. J. Earth Sci. (Geol. Rundsch.), 102: 783-811.

Bortolotti V., Kodra A., Marroni M., Mustafa F., Pandolfi L., Principi G. and Saccani E., 1996. Geology and petrology of ophiolitic sequences in the Mirdita region (Northern Albania). Ofioliti, 21: 3-20.

Chiari M., Baumgartner P.O., Bernoulli D., Bortolotti V., Marcucci M., Photiades A., Principi G., 2013. Late Triassic, Earéy and Middle Jurassic Radiolaria from ferromanganese-chert 'nodules' (Angelokastron, Argolis, Greece): evidence for prolongated radiolarite sedimentation in the Maliac-Vardar Ocean. Facies, 59: 391-424.

Chiari M., Bortolotti V., Marcucci M., Photiades A. and Principi G., 2003. The Middle Jurassic siliceous sedimentary cover at the top of the Vourinos Ophiolite (Greece). Ofioliti, 28: 95-103.

Chiari M., Bortolotti V., Marcucci M., Photiades A., Principi G. and Saccani E., 2012. Radiolarian biostratigraphy and geochemistry of the Koziakas massif ophiolites (Greece). Bull. Soc. Géol. Fr., 183 (4): 287-306.

Chiari M., Djerić N., Garfagnoli F., Hrvatović H., Krstić M., Levi N., Malasoma A., Marroni M., Menna F., Nirta G., Pandolfi L., Principi G., Saccani E., Stojadinović U. and Trivić B., 2011. The geology of the Zlatibor-Maljen area (western Serbia): a geotraverse across the ophiolites of the Dinaric-Hellenic collisional belt. Ofioliti, 36: 139-166.

Ćirić B. and Karamata S. 1960. L'évolution du magmatisme dans le géosynclinal dinaridique du Mésozoïque au Cenozoïque. Bull. Soc. Géol. Fr., 7 (2): 376-378.

Dimitrijević M.D., 1997. Geology of Yugoslavia. Geol. Inst. GEMINI, Belgrade, 187 pp.

Dimitrijević M.D. and Dimitrijević M.N., 1973. Olistostrome mélange in the Yugoslavian Dinarides and Late Mesozoic plate tectonics. J. Geol., 81: 328-340.

Dimitrijević M.N., Dimitrijević M.D., Karamata S., Sudar M., Gerzina N., Kovács S., Dosztály L., Gulácsi Z., Less Gy. and Pelikán P., 2003. Olistrotrome/mélanges - an overview of the problems and preliminary comparison of such formations in Yugoslavia and NE Hungary. Slovak Geol. Mag., 9: 3-21.

Djerić N. and Gerzina N., 2008. Late Triassic radiolarians from the Ovčar-Kablar gorge (SW Serbia). Ann. Géol. Pénins. Balcan., 69: 39-47.

Djerić N., Gerzina N. and Simić D., 2010. Middle Jurassic radiolarian assemblages from Zlatar Mt. (SW Serbia). Ann. Géol. Pénins. Balcan., 71: 119-125.

Ferrière J., Baumgartner P.O. and Chanier F., 2016. The Maliac Ocean: the origin of the Tethyan Hellenic ophiolites. Intern. J. Earth Sci. (Geol. Rundsch.), 105: 1941-1963.

Ferrière J., Chanier F. and Ditbanjong P., 2012. The Hellenic ophiolites: eastward or westward obduction of the Maliac Ocean, a discussion. Intern. J. Earth Sci. (Geol. Rundsch.), 101: 1559-1580.

Gawlick H.J., Frisch W., Hoxha L., Dumitrica P., Krystyn L., Lein R., Missoni S. and Schlagintweit F., 2008. Mirdita Zone ophiolites and associated sediments in Albania reveal Neotethys Ocean origin. Intern. J. Earth Sci., 97: 865-881.

Gawlick H. J., Missoni S., Suzuki H., Sudar M., Lein R. and Jovanović D., 2016. Triassic radiolarite and carbonate components from a Jurassic ophiolite mélange (Dinaridic Ophiolite Belt). Swiss J. Geosci., 109: 473-494.

Gawlick, H.J., Sudar, M., Suzuki, H., Đerić, N. Missoni, S. Lein, R. and Jovanović D., 2009. Upper Triassic and Middle Jurassic radiolarians from the ophiolitic mélange of the Dinaric Ophiolite Belt, SW Serbia. N. Jahrb. Geol. Paläont. Abhandl., 253: 293-311.

Goričan Š., Halamić J., Grgasović T. and Kolar-Jurkovšek T., 2005. Stratigraphic evolution of Triassic arc-backarc system in northwestern Croatia. Bull. Soc. Géol. Fr., 176: 3-22.

Goričan Š., Karamata S. and Botočanin-Srečković D., 1999. Upper Triassic (Carnian-Norian) radiolarians in chert of Sijenica (SW Serbia) and the time span of the oceanic realm ancestor of the Dinaridic Ophiolite Belt. Bull. T. 119, Cl.. Sci. Nat., Acad. Serb. Sci. Arts, 39: 141-150.

Halamić J. and Goričan Š., 1995. Triassic radiolarites from Mts. Kalnik and Medvednica (Northwestern Croatia). Geol. Croat., 48: 129-146.

Halamić J., Goričan Š., Slovenec D. and Kolar-Jurkovšek T., 1999. A Middle Jurassic Radiolarite-Clastic Succession from the Medvednica Mt. (NW Croatia). Geol. Croat., 52 (1): 29-57.

Halamić J., Slovenec D. and Kolar-Jurkovšek T. 1998. Triassic pelagic limestones in pillow lavas in the Orešje Quarry near Gornje Bistra, Medvednica Mt. (Northwest Croatia). Geol. Croat., 51: 33-45.

Jones G. and Robertson A.H.F., 1991. Tectono-stratigraphy and evolution of the Mesozoic Pindos ophiolite and related units, northwestern Greece. J. Geol. Soc. London, 148: 267-288.

Karamata S., 2006. The geological development of the Balkan Peninsula related to the approach, collision and compression of Gondwana and Eurasian units. In: A.H.F. Robertson and D. Mountrakis (Eds.), Tectonic development of the Eastern Mediterranean Region. Geol Soc London Spec Publ, 260: 155-178.

Karamata S., Knežević V. and Cvetković V., 2000. Petrology of the Triassic basaltoid rocks of Vareš (Central Bosnia). Acta Geol. Hung., 43: 1-14.

Leterrier J., Maury R.C., Thonon P., Girrard D. and Marchal M., 1982. Clinopyroxene composition as a method of identification of the magmatic affinities of paleovolcanic series. Earth Planet. Sci. Lett., 59: 139-154.

Lugović B., Altherr R., Raczek I., Hofmann A.W. and Majer V., 1991. Geochemistry of peridotites and mafic igneous rocks from the Central Dinaridic Belt, Yugoslavia. Contrib. Mineral. Petrol., 106: 201-216.

Lugović B., Slovenec D., Schuster R., Schwarz W.H. and Horvat M., 2015. Petrology, geochemistry and tectono-magmatic affinity of gabbroic olistoliths from the ophiolite mélange in the NW Dinaric-Vardar ophiolite zone (Mts. Kalnik and Ivanščica, North Croatia). Geol. Croat., 68: 25-49.

Marcucci M., Kodra A., Pirdeni A. and Gjata T., 1994. Radiolarian assemblages in the Triassic and Jurassic cherts of Albania. Ofioliti, 19: 105-114.

Morimoto N., 1988. Nomenclature of Pyroxenes. Am. Miner., 73: 1123-1133.

Obradović J. and Goričan Š., 1988. Siliceous deposits in Yugoslavia: occurences, types and ages. In: J. Hein and J. Obradović (Eds.), Siliceous deposits of the Thetys and Pacific regions. Springer-Verlag, New York, p. 51-64.

O'Dogherty L., Bill M., Goričan Š., Dumitrica P. and Masson H., 2006. Bathonian radiolarians from an ophiolitic mélange of the Alpine Tethys (Gets Nappe, Swiss-French Alps). Micropaleontology, 51: 425-485.

O'Dogherty L., Carter E.S., Dumitrica P., Goričan Š., De Wever P., Bandini A.N., Baumgartner P.O. and Matsuoka A., 2009. Catalogue of Mesozoic radiolarian genera. Part 2: Jurassic - Cretaceous. In: L. O'Dogherty, Š. Goričan and P. De Wever (Eds.), Catalogue of Mesozoic radiolarian genera. Geodiver., 31: 271-356.

O'Doghetry L., Gorican S. and Gawlick H.J., 2017. Middle and Late Jurassic radiolarians form the Neotethys suture in the Eastern Alps. J. Paleont., 91: 25-72.

Pamić J., Tomljenović B. and Balen D., 2002. Geodynamic and petrogenetic evolution of Alpine ophiolites from central and NW Dinarides: an overview. Lithos, 65: 113-142.

Pe-Piper G., 1998. The nature of Triassic extension-related magmatism in Greece: evidence from Nd and Pb isotope geochemistry. Geol. Mag., 135: 331-348.

Prela M., Chiari M. and Marccuci M., 2000. Jurassic radiolarian biostratigraphy of the sedimentary cover of ophiolites in the Mirdita Area, Albania: new data. Ofioliti, 25: 55-62.

Robertson A.H.F., 2012. Late Palaeozoic-Cenozoic tectonic development of Greece and Albania in the context of alternative reconstructions of Tethys in the Eastern Mediterranean region. Intern. Geol. Rev., 54: 373-454.

Robertson A.H.F.., Karamata S. and Šarić K., 2009. Ophiolites and related geology of the Balkan region. Lithos, 108: 1-36.

Robertson A.H.F., Trivić B., Đerić N. and Bucur I.I., 2013. Tectonic development of the Vardar ocean and its margins: Evidence from the Republic of Macedonia and Greek Macedonia. Tectonophysics, 595-596: 25-54.

Saccani E., 2015. A new method of discriminating different types of post-Archean ophiolitic basalts and their tectonic significance using Th-Nb and Ce-Dy-Yb systematics. Geosci. Front., 6: 481-501. http://dx.doi.org/10.1016/j.gsf.2014.03.006.

Saccani E. and Photiades A., 2005. Petrogenesis and tectonomagmatic significance of volcanic and subvolcanic rocks in the Albanide-Hellenide ophiolitic melanges. Isl. Arc, 14: 494-516.

Saccani E., Beccaluva L., Photiades A. and Zeda O., 2011. Petrogenesis and tectono-magmatic significance of basalts and mantle peridotites from the Albanian-Greek ophiolites and sub-ophiolitic mélanges. New constraints for the Triassic-Jurassic evolution of the Neo-Tethys in the Dinaride sector. Lithos, 124: 227-242.

Saccani E., Dilek Y., Marroni M. and Pandolfi L., 2015. Continental margin ophiolites of Neotethys: Remnants of ancient Ocean-Continent Transition Zone (OCTZ) lithosphere and their geochemistry, mantle sources and melt evolution patterns. Episodes, 38: 230-249, doi: 10.18814/epiiugs/2015/v38i4/82418.

Saccani E., Dilek Y. and Photiades A., 2017. Time-progressive mantle - melt evolution and magma production in a Tethyan marginal sea: A case study of the Albanide-Hellenide Ophiolites. Lithosphere, Spec. Issue, in press.

Saccani E., Padoa E. and Photiades A., 2003. Triassic mid-ocean ridge basalts from the Argolis Peninsula (Greece): new constraints for the early oceanization phases of the Neo-Tethyan Pindos basin. In: Y. Dilek and P.T. Robinson (Eds.), Ophiolites in Earth history. Geol. Soc. London, Spec. Publ., 218: 109-127.

Schmid S.M., Bernoulli D., Fugenschuh B., Matenco L., Schefer S., Schuster R., Tischler M. and Ustaszewski K., 2008. The Alpine-Carpathian-Dinaridic orogenic system: correlation and evolution of tectonic units. Swiss J. Geosci., 101: 139-183.

Šegvić B., 2010. Petrologic and geochemical characteristics of the Krivaja-Konjuh ophiolite complex (NE Bosnia) - petrogenesis and regional geodynamic implications. Ph.D. thesis, Univ. Heidelberg, Germany, 301 pp.

Šegvić B., Kukoč D., Dragičević I., Vranjković A., Brčić V., Goričan Š., Babajić E. and Hrvatović H., 2014. New record of Middle Jurassic radiolarians and evidence of Neotethyan dynamics documented in a mélange from the Central Dinaridic Ophiolite Belt (CDOB, NE Bosnia and Herzegovina). Ofioliti, 39: 31-41.

Šegvić B., Lugović B., Slovenec D. and Meyer H.P. 2016. Mineralogy, petrology and geochemistry of amphibolites from the Kalnik Mt. (Sava unit, North Croatia): Implications for the evolution of north-westernmost part of the Dinaric-Vardar branch of Mesozoic Tethys. Ofioliti, 41: 35-58.

Slovenec D. and Lugović B., 2009. Geochemistry and tectonomagmatic affinity of mafic extrusive and dyke rocks from the ophiolite mélange of the SW Zagorje-Mid-Transdanubian zone (Mt. Medvednica, Croatia). Ofioliti, 34: 63-80.

Slovenec D. and Lugović B., 2012. Evidence of the spreading culmination in the Eastern Tethyan Repno oceanic domain, assessed by the petrology and geochemistry of the N-MORB extrusive rocks from the Mt. Medvednica ophiolite mélange (NW Croatia). Geol. Croat., 65: 435-446.

Slovenec D., Lugović B., Hans-Peter Meyer H.-P. and Garapić Šiftar G., 2011. Tectono-magmatic correlation of basaltic rocks from ophiolite mélanges at the north-eastern tip of the Sava-Vardar suture zone, Northern Croatia, constrained by geochemistry and petrology. Ofioliti, 36: 77-100.

Slovenec D., Lugović B. and Vlahović I., 2010. Geochemistry, petrology and tectonomagmatic significance of basaltic rocks from the ophiolite mélange at the NW External-Internal Dinarides junction (Croatia). Geol. Carpat., 61: 273-292.

Šmuc A. and Goričan S., 2005: Jurassic sedimentary evolution of a carbonate platform into a deep-water basin, Mt. Mangart (Slovenian-Italian border). Riv. It. Pleont. Strat., 111 (1): 45-70.

Spray J.G., Bébien J., Rex D.C. and Roddick J.C., 1984. Age constraints on the igneous and metamorphic evolution of the Hellenic-Dinaric ophiolites. In: J.E. Dixon et al. (Eds.), The geological evolution of the Eastern Mediterranean. Geol. Soc. London Spec. Publ., 17: 619-627.

Sun S.S. and McDonough W.F., 1989. Chemical and isotopic systematics of oceanic basalts: implications for mantle composition and processe. In: A.D. Saunders and M.J. Norry (Eds.), Magmatism in oceanic basins. Geol. Soc. London Spec. Publ., 42: 313-345.

Trubelja F., Marching V., Burgath K. P. and Vujovic Z., 1995. Origin of the Jurassic Tethyan ophiolites in Bosnia: A geochemical approach to tectonic setting. Geol. Croat., 48: 49-66.

Ustaszewski K., Schmid S., Lugović B., Schuster R., Schaltegger U., Bernoulli D., Hottinger L., Kounov A., Fügenschuh B. and Schefer S., 2009. Late Cretaceous intra-oceanic magmatism in the internal Dinarides (northern Bosnia and Herzegovina): Implications for the collision of the Adriatic and European plates. Lithos, 108: 106-125.

Ustaszewski K., Kounov A., Schmid S., Schaltegger U., Krenn E., Frank W. and Fügenschus B., 2010. Evolution of the Adria-Europe plate boundary in the northern Dinarides: From continent-continent collision to back-arc extension. Tectonics, 29: 1-34.

Vishnevskaya V.S., Djeric, N. and Zakariadze G.S., 2009. New data on Mesozoic radiolaria of Serbia and Bosnia, and implications for the age and evolution of oceanic volcanic rocks in the Central and Northern Balkans. Lithos, 108: 72-105.

Winchester J.A. and Floyd P.A., 1977. Geochemical discriminations of different products using immobile elements. Chem. Geol., 20: 325-343.

Wood D.A., 1980. The application of a Th-Hf-Ta diagram to problems of tectonomagmatic classification and establishing the nature of crustal contamination of basaltic lavas of the British Tertiary volcanic province. Earth Planet. Sci. Lett., 50: 11-30.

Received, May 16, 2017
Accepted, November 9, 2017

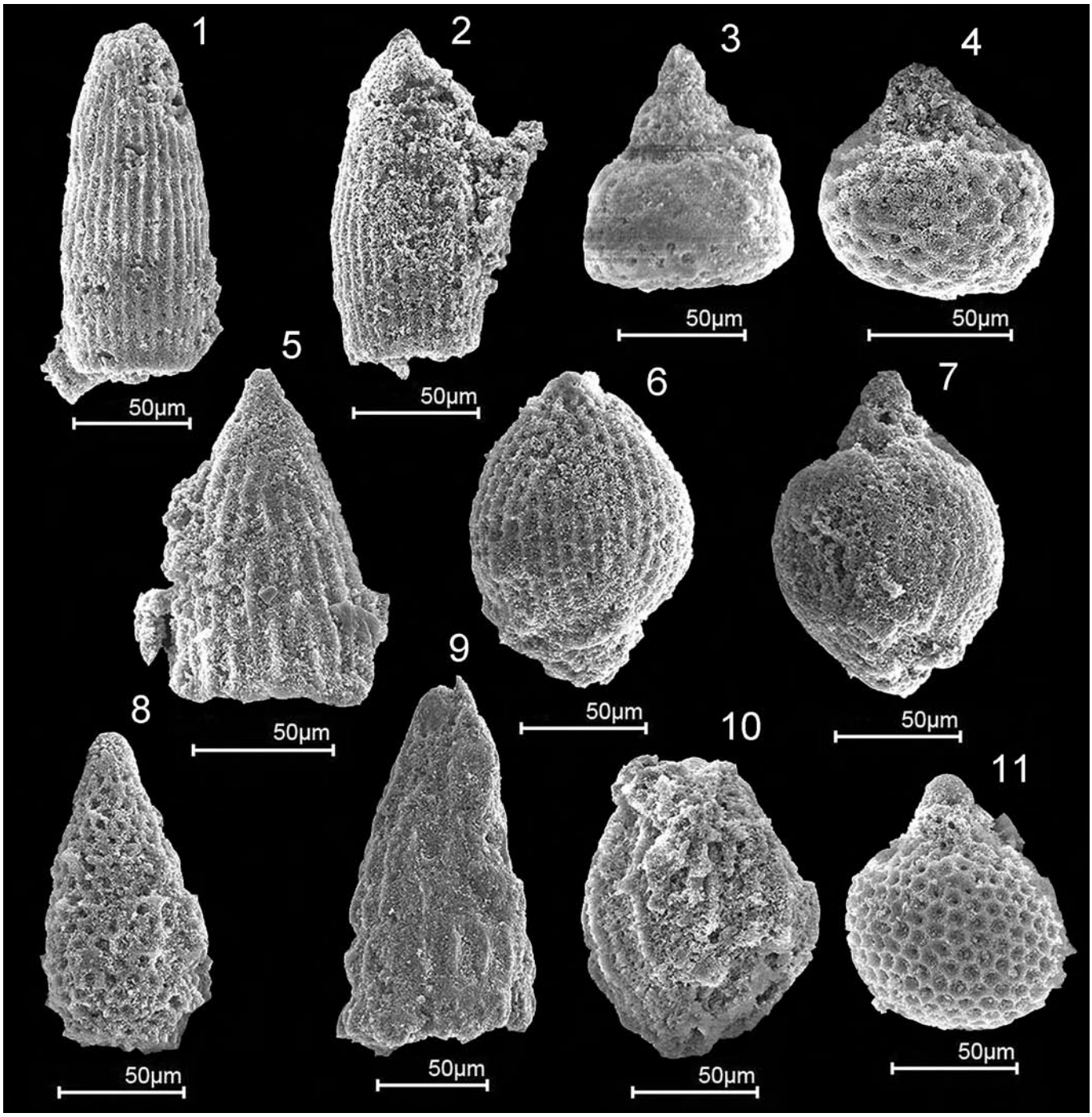

Plate 1 - Radiolarians from sample doz-10. For each specimen SEM number is indicated.
1) *Archaeodictyomitra* sp. cf. *A. prisca* Kozur and Mostler, 100212; 2) *Archaeodictyomitra* sp. cf. *A. rigida* Pessagno, 100201, 3) *Eucyrtidiellum pustulatum* Baumgartner, 100202; 4) *Hemicryptocapsa* sp. cf. *H. yaoi* (Kozur), 100210; 5) *Hsuum* sp., 100207; 6) *Striatojaponocapsa conexa* (Matsuoka), 100205; 7) *Striatojaponocapsa* (?) sp., 100203; 8) *Takemuraella* sp., 100220; 9) *Transhsuum* sp. cf. *T. crassum* Chiari, Marcucci and Prela, 100221; 10) *Unuma* sp. cf. *U. gordus* Hull, 100213; 11) *Zhamoidellum* sp. cf. *Z. ventricosum* Dumitrica, 100208.